(15) "Multiref 901, Instruction Manual", Optilab AB, Box 138, S-162 12 Vällingby 1, Sweden.
(16) F. Candau, J. Francois and H. Benoît, *Polymer*, **15**, 626 (1974).
(17) L. Carlson, *Histochemie*, **21**, 289 (1970).
(18) L. Carlson, Optilab AB, Sweden, private communication, 1976.
(19) F. S. Crawford Jr., "Waves", Berkeley Physics Course, Vol. 3, McGraw-Hill, New York, N.Y., 1968, pp 394–436.
(20) W. Nebe, "Comprehensive Analytical Chemistry", Vol. 8, G. Svehla, Ed., Elsevier, Amsterdam, 1977, p 423.
(21) I. Brandrup and E. H. Immergut, "Polymer Handbook", Interscience, New York, N.Y., 1966, p IV-302.
(22) F. R. Senti, N. N. Hellman, N. H. Ludwig, G. E. Babcock, R. Tobin, C. A. Glass, and B. L. Lamberts, *J. Polym. Sci.*, **17**, 527 (1955).
(23) C. F. Snyder, H. S. Isbell, M. R. Dryden, and N. B. Holt, *J. Res. Natl. Bur. Stand.*, **53**, 3 (1954), RP 2525.
(24) I. Brandrup and E. H. Immergut, "Polymer Handbook", Wiley-Interscience, New York, N.Y., 1975, p VI-47.
(25) L.-O. Sundelöf and P. H. Norberg, unpublished work, Institute of Physical Chemistry, Uppsala, Sweden, 1964. (See also P. H. Norberg and L.-O. Sundelöf, *Makromol. Chem.*, **77**, 77(1964).)
(26) F. Daniels and R. A. Alberty, "Physical Chemistry", J. Wiley & Sons Inc., New York, N.Y., 1967, p 690.
(27) I. M. Kolthoff, E. B. Sandell, E. J. Meehan, and S. Bruckenstein, "Quantitative Chemical Analysis", Macmillan Company, London, 1969, p 1007.

X-ray Photoelectron Spectroscopy of Alkylamine–Silanes Bound to Metal Oxide Electrodes

P. R. Moses, Larry M. Wier,[1] John C. Lennox,[2] H. O. Finklea, J. R. Lenhard, and Royce W. Murray*

Kenan Laboratories of Chemistry, University of North Carolina, Chapel Hill, North Carolina 27514

ESCA results are presented for SnO₂, RuO₂, TiO₂, and Pt/PtO oxide electrodes silanized with trialkoxyalkylamine–silanes. Observations include effects of reaction conditions, assay of the fraction of amine-like surface nitrogen, assay of N/Si surface atom ratios, O 1s spectra, and fluoride dopant depth profile in SnO₂. The silanized surfaces are amine-like but also exhibit other chemical features. The implications of various alkylamine–silane surface structures on electrochemical applications are discussed.

Trialkoxyalkylamine–silanes react with the surfaces of several metal oxides which are useful as electrodes in electrochemical experiments. These include highly doped SnO_2 (*1*), RuO_2 (*2*), and "PtO" electrochemically formed on Pt metal (Pt/PtO electrode) (*3*). Carbon electrodes also react with organosilanes (*4*). Binding of the alkylamine–silanes to these surfaces is a first step toward immobilizing various reagents on the chemically modified electrodes. Immobilization of several reversibly reduced redox reagents via amide bond formation on alkylamine–silanized RuO_2, Pt/PtO, and SnO_2 electrodes has been described (*2, 3, 5*). Electron transfer reactions between immobilized redox reagents and the electrode surface may be sensitive to the connecting alkylamine–silane layer's structure, composition, and stereochemistry. We report here a number of experiments, principally using ESCA (Electron Spectroscopy for Chemical Analysis), directed at these aspects of the metal oxide/alkylamine–silane interface.

Our (*1, 6*) and others' (*7*) previous pictures of silanized metal oxide electrode surfaces were simplified versions of interfaces which are more complex in a variety of ways. The present study aims at furthering our understanding of the structure and composition of the metal oxide/alkylamine–silane interface. Parts of a model have been discussed (*5, 8*). The trialkoxyalkylamine–silanes employed are 3-(2-aminoethyl-amino)propyltrimethoxysilane (*en* silane) and 3-amino-propyltriethoxysilane (*PrNH₂* silane), and the metal oxide electrodes are SnO_2, RuO_2, TiO_2, and Pt/PtO. Continuing study of the alkylamine–silane and other silanized interfaces will doubtless in the future evoke additional understandings. In particular, we note that the four metal oxide surfaces have not been subjected with equal thoroughness to all different types of experiments discussed. In many respects the four metal oxides appear to behave similarly, but some intrinsic differences beyond those noted probably exist. Presumption of general similarity must be regarded for the present as a crude approximation.

The observations fall into four major categories: (i) effects of reaction conditions, (ii) assay of the fraction of surface nitrogen which reacts in a normal, "amine-like" manner, (iii) assay of bound silane composition through N/Si atom ratios, and (iv) O 1s ESCA spectra of the silanized surfaces. We also describe a depth profile of fluoride dopant in SnO_2 electrodes, and a lack of success in achieving useful amidizations of alkylamine-silanized carbon electrodes (*4*).

Alkylamine–silanes are widely employed for the chemical modification of various silica and alumina surfaces used in bonded phase liquid chromatography (*9–11*), affinity chromatography (*12*), trace metal analysis (*13, 14*), immobilization of transition metal catalysts (*15*), and in adhesion technology (*16*), among others. While we have carried out few experiments on nonconducting oxides, our model appears consistent with what is known about alkylamine-silanized silica and alumina, and adds by inference some additional features.

EXPERIMENTAL

Metal Oxide Electrodes. TiO_2 was prepared in polycrystalline thin film form by chemical vapor deposition according to Bard (*17*) or by simply heating Ti metal in a Bunsen burner flame. SnO_2 films on glass (commercially prepared) (*1*), spray-atomized RuO_2 films on Ti (*2*) and Pt/PtO electrodes (*3*) were obtained as previously described.

Chemicals. The *PrNH₂* silane (3-aminopropyltriethoxysilane) and *en* silane (3-(2-aminoethylamino)propyltrimethoxysilane) (PCR Chemical Co.), earlier used as received, are now routinely vacuum distilled upon ESCA evidence of polymer contaminant. Nitrobenzoyl and fluorobenzoyl chlorides were from Aldrich. Benzene was dried over sodium.

[1] Present address, Department of Chemistry, Union College, Schenectady, N.Y. 12308.
[2] Present address, Department of Chemistry, University of Arkansas, Fayetteville, Ark. 72701.

ESCA. X-ray (Mg anode) photoelectron spectra were obtained with a DuPont 650B electron spectrometer (1). In later experiments the data acquisition and manipulation features of this instrument were modified with a microprocessor system to be described elsewhere (18). Typical vacuum level was 1×10^{-7} Torr. A C 1s contaminant line was reproducibly present. B.E. of other elements are referenced to the C 1s line taken as 285.0 eV. Sputtering experiments were typically carried out with 1.5 keV and 35 mA Ar^+ beam current. As samples for electron spectroscopy were necessarily exposed to the atmosphere during the synthetic preparation, care was taken to avoid contaminant sources particularly of Si and N, and to check for these elements with control samples. Si remained a problem with SnO_2 electrodes as discussed in the text. Possibly excepting Pt/PtO, the metal oxides do not tend to adsorb alkylamines (probable silane reagent contaminant) from benzene control solutions.

Silanization Reaction Conditions. Procedures identified previously as reaction Methods A, C, and D (1, 6) are: Method A involves prolonged reflux of the metal oxide electrode in a 10% silane solution in benzene or xylene. Method C carries out the reaction in a glove box (Vacuum Atmospheres) or in syringe cap vials in 1–5% silane solutions in benzene at room temperature for 5–60 min. Method D uses typically 1% silane in 6 °C benzene for periods ranging from 10 s to 10 min. Silanized samples are washed very thoroughly with dry benzene before removal from the reaction flask, to avoid contact of any silane-containing solvent with atmospheric moisture, and then with methanol in many cases. An additional silanization procedure (Method E) has undergone preliminary tests; in this method the sample is reacted with silane vapor in an apparatus maintaining the sample at ca. 60 °C for 12 h. We have little ESCA data on samples prepared by Method E, but silanization does occur on RuO_2, and amidization with 3,5-dinitrobenzoyl chloride yields the expected surface electrochemistry (2).

Amidization Conditions. Reaction of 3,5-dinitrobenzoyl chloride with silanized metal oxide samples has been carried out using a range of conditions. Typical solution concentration is 0.05 M in $CHCl_3$ solvent, the reaction time ranges from 10–60 min, and temperature from room to ca. 60 °C. In some cases a catalyst base such as 2,6-lutidene or 1,8-dimethylaminonaphthalene is added, but care must be taken in the washing procedure that this nitrogen-containing material is adequately washed from the sample. The latter base, for instance, adsorbs rather strongly on RuO_2 surfaces, and its use there is undesirable for experiments involving N 1s ESCA spectra.

RESULTS

Effects of Reaction Conditions. Reaction conditions for metal oxide silanizations include the (i) pretreatment of the metal oxide surface, (ii) conditions under which the silane is contacted with the surface and excess rinsed from the surface, and (iii) conditions under which the freshly silanized surface is handled en route to subsequent measurements or chemical reactions with the alkylamine moiety. We will discuss each of these in turn.

Pretreatment. Pretreatment is known to be important for chemical modification of SiO_2 surfaces. At room temperature only ca. 50% of the surface oxygens are thought to achieve a hydroxylated (–SiOH) state (19, 20). Except under highly acidic, basic, or dehydrating conditions, infrared measurements on TiO_2 (21), and SnO_2 (22) powders indicate that the surface lattice oxygens are predominantly in a hydroxylated (–MOH) state. Strongly dehydrating conditions are required to reduce O–H stretching intensities with generation, presumably of oxygen-bridged M–O–M sites. The –MOH site should constitute the reactive site for the alkoxysilane groups. Thus it is not greatly surprising that no influence of pretreatment, under conditions ranging from hot concentrated HCl to 450 °C drying followed by re-exposure to air, was discerned in previous (1) and ensuing studies of SnO_2.

Pretreatment conditions employed thus far for RuO_2 and TiO_2 films have been governed by considerations of producing
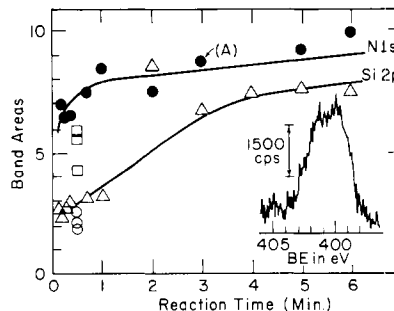

Figure 1. Reaction kinetics of *en* silane in 6 °C benzene with SnO_2. Reaction quenched with benzene rinse. (– ● –) I_{N1s} for 1% silane solution, (□) $I_{N\ 1s}$ for 0.1% solution, (O) for 0.001% solution; (–△–) $I_{Si\ 2p}$ for 1% solution. N 1s spectral inset for data point "A"

adherent and properly conducting or doped materials in the film preparation process itself. Exposure to laboratory air is permitted before silanization. These surfaces are reactive toward the silane reagents and we have no data suggesting that they are not extensively hydroxylated.

Pretreatment of the approximate monolayer of oxide on Pt/PtO electrodes has been restricted to low temperature oven drying (50 °C) to protect the layer. The silanization reaction is sensitive to the conditions of the electrochemical preparation of the oxide layer (4).

Overall, while detailed investigation of pretreatment effects is incomplete, we have not yet, except for perhaps Pt/PtO, discerned pretreatment to be as important a reaction condition variable as those described below.

Silanization Reaction Conditions. The significance of anhydrous reaction conditions for the silanization process has been emphasized (1). Growth of three-dimensional siloxane polymer can be substantially avoided under anhydrous conditions (6). Of the various reaction methods employed (see Experimental), the earliest (Method A) (1) is unnecessarily forcing for the metal oxides considered here. The room temperature Method C is convenient and is thought to yield a limiting coverage as "monolayer" to distinguish it from "multilayer" (as with siloxane polymer growth). We emphasize that this is a reaction site-limited coverage and may not be the same as a coverage limited by the molecular dimension of the alkylamine–silane. Molecular dimension-limited coverages are those typical in Langmuir–Blodgett experiments (23).

The very mild Method D was originally investigated as a strategy to achieve coverages less than the reaction site-limited value. Figure 1 shows N 1s and Si 2p ESCA band intensities on SnO_2 surfaces reacted with 6 °C, 1% *en* silane solutions for various times. The time dependence of the two elements is different; we believe the N 1s data represent alkylamine–silane coverage more accurately. The Si 2p data will be discussed later. The N 1s band is a doublet due to free base and protonated amine (N and NH^+) forms (1); relative N/NH^+ intensity is not a function of reaction time. The Figure 1 data are total N 1s intensity, which rises quite rapidly to a gradually sloping plateau. For a 3–6 min reaction time, the N 1s intensity achieved is within 20% of the average intensity (1) for *en* silane reacted successfully with SnO_2 using Method A.

The N 1s data of Figure 1 show that achieving less than limiting coverages of *en* silane on SnO_2 using 1% silane solutions with Method D requires inconveniently short reaction times. Lowering the *en* silane concentration can be an effective tactic for a 30-s reaction period, as illustrated by Figure 1 for 0.1% and 0.001% solutions. The latter corresponds to about 25% coverage. The reproducibility of such low coverage experiments is not very good, and comparable experiments have not yet been conducted on the other metal oxides.
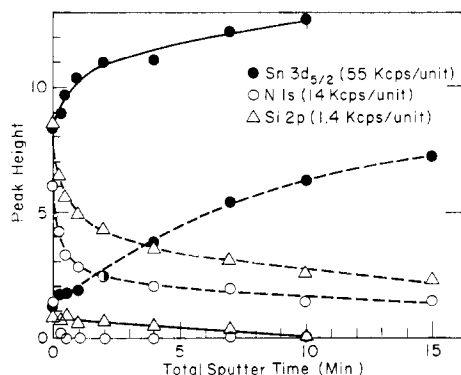
Figure 2. 1.5 keV Ar$^+$ sputter of SnO$_2$/en electrodes prepared by Method D (——) and by a Method A experiment in which polymer formed (- - - -)
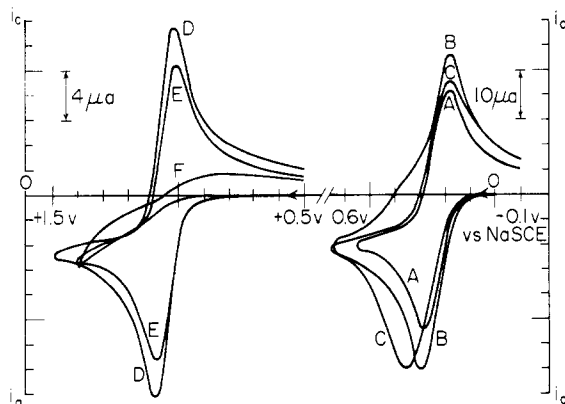

Figure 3. Cyclic voltammograms on SnO$_2$ (Curves A, D), SnO$_2$/en prepared with Method D (Curves B, E), and SnO$_2$/en prepared with Method A (Curves C, F). Same electrode preparation as used for data of Figure 2 but different specimens. Curves A–C: ca. 2 mM ferrocyanide in 0.1 M KCl and pH 2.4, 0.5 M glycine buffer. 200 mV/s. Curves D–F: 1 mM Ru(bpy)$_3$(ClO$_4$)$_2$ in 0.18 M H$_2$SO$_4$, 0.1 M KCl. 200 mV/s

Electrodes with sub-monolayer silane coverage may be useful for study of steric aspects of redox couples (2, 24) immobilized on electrodes using alkylamine–silane chemistry.

The incidence of poor electrode preparations in which siloxane polymer-forming misadventures occur is much higher with Method A than the milder Methods C and D. For example, in a comparison preparation of SnO$_2$/en electrodes using Methods A and D, the Method A electrode showed evidence of polymer formation by greatly reduced Sn 3d$_{5/2}$ band intensity ($I_{silane}/I_{unreact}$ = 0.09 vs. 0.68 on the Method D electrode) and prolonged N 1s and Si 2p signals upon sputtering, as shown in Figure 2. On method D (and C) electrodes, N 1s disappears after a few seconds of sputtering, and Si 2p a little more slowly. Both bands were persistent on the polymer-coated Method A electrode, and Sn 3d$_{5/2}$ and O 1s intensity remained low after several minutes of erosion.

We presumed earlier (1) that electrochemical properties would be quite sensitive to siloxane polymer formation. Figure 3 compares cyclic voltammetry of aqueous ferrocyanide and Ru(bpy)$_3$$^{2+}$ on native SnO$_2$ and on the Method A and D SnO$_2$/en. The reversibility of both electrode reactions on native SnO$_2$ and Method D-SnO$_2$/en is quite similar. The oxidation of Ru(bpy)$_3$$^{2+}$ on the polymer-bearing Method A-SnO$_2$/en is poorly defined, very irreversible, with small currents, but the ferrocyanide reaction is only mildly irreversible (Curve C). The negatively charged Fe(CN)$_6$$^{4-}$ apparently readily penetrates the siloxane film, which at the solution pH employed should bear positive ammonium sites. Ru(bpy)$_3$$^{2+}$ tends to be excluded because of either its charge or larger size. This comparison shows that electrochemical

properties are not necessarily good criteria to distinguish polymer-coated from monolayer-coated electrodes.

Gleria and Memming (25) have reported abnormally small, nondiffusion controlled currents for aqueous Ru(bpy)$_3$$^{2+}$ oxidation at highly doped SnO$_2$ in aqueous acid, interpreting this as Ru(bpy)$_3$$^{2+}$ adsorption on the SnO$_2$ surface. In our experiments, we saw no evidence for adsorption by ESCA of Ru(bpy)$_3$$^{2+}$-exposed SnO$_2$. Cyclic voltammetric $i_p/v^{1/2}$ of aqueous Ru(bpy)$_3$$^{2+}$ solutions is constant over 5–500 mV/s sweep rate. The diffusion coefficient calculated from the $i_p/v^{1/2}$ data has a normal value (6 × 10^{-6} cm^2/s).

Post-Silanization Treatment. If the reaction of the three alkoxysilane functions present on PrNH$_2$ and en silanes with the metal oxide surface is incomplete, "dangling" alkoxysilane groups may exist on the electrode surface after silanization is terminated. The fate of these dangling groups, as determined by handling of the silanized electrode, may influence the behavior of the alkylamine–silane/metal oxide interface in subsequent measurements or reactions of the amine sites. The reaction of the trialkoxyalkylamine–silane with hydroxylated metal oxide surface can be written
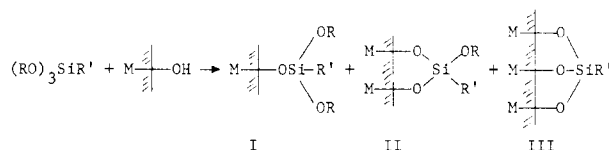
where Structures I, II, and III represent different degrees of coupling and R′ is the alkylamine or some other group. Published descriptions of the relative proportions of these structures are both sparse and generally nonquantitative, as analysis for them is a difficult problem. In reactions of chloromethylsilanes with silica surfaces, Structure I is often presumed without justification other than probable bond strain in Structure III plus incomplete SiO$_2$ surface hydroxylation. Residual Si-Cl has been detected after silica reaction with dimethyldichlorosilane (20). An average of two Al-O-Si bonds per silane (e.g., Structure II) was reported (26) after reaction of a trichlorosilane with alumina. After reaction of dimethyldichlorosilane with tin(IV) oxide gel, Harrison and Thornton (27) showed that the silanized material reacts with acetic acid vapor to yield infrared bands assignable to a silyl ester, which was hydrolyzed slowly by water with appearance of spectral features attributed to -SiOH groups. Examination of SnO$_2$ films by inelastic tunneling spectrometry following reaction with triethoxyvinylsilane has produced evidence for dangling ethoxysilane groups (28). Similarly, Raman bands assigned to Si-Cl have been observed on SnO$_2$ following reaction with 3-chloropropyltrichlorosilane (29). Thus some evidence exists for Structures I and II and for dangling reactive groups on silanized surfaces, but none for Structure III.

Accordingly, it seems reasonable to assume in silanizations of metal oxide electrodes with trialkoxyalkylamine–silanes that the surface products contain, or perhaps are predominantly, Structures I and II. Post-silanization handling of these surfaces can be in three modes. Assuming for the discussion Structure II, the post-silanization environment of the surface can be maintained in an anhydrous and aprotic state, to attempt to preserve the dangling alkoxysilane. Alternatively, the surface can be deliberately exposed to moisture, hydrolyzing the alkoxysilane group to an -SiOH function as in Structure IV
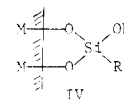

Thirdly, thermal curing can be used to attempt two-di-

Table I. Assay of Active Amine

Acid–Base Assay

Expt	Electrode[a]	Treatment[b]	$I_{N\ 1s(400)}/I_{N\ 1s(401.5)}$[c], %	Active amine[d], %
I-1	SnO2/PrNH2	pH 10 wash	76/24	
		0.05 M HCl wash	58/42	16
I-2	SnO2/en	pH 10 wash	72/28	
		0.05 M HCl wash	41/59	31
I-3	RuO2/en	pH 10 wash	61/37	
		0.05 M HCl wash	39/63	26

Amidization Assay

Expt	Electrode[a]	Treatment[b]	$\dfrac{I_{N\ 1s(406.5)}}{I_{N\ 1s(Amine\ +\ amide)}}$	$\dfrac{I_{F\ 1s(687)}}{I_{N\ 1s(Amine\ +\ amide)}}$	Active amine[e], %
I-4	SnO2/PrNH2	4-(NO2)PhCOCl	0.20,[f] 0.27		20,[f] 27
I-5	SnO2/PrNH2	3,5-(NO2)2PhCOCl	0.13		6
I-6	SnO2/PrNH2	4-FPhCOCl		0.53	22
I-7	SnO2/en	4-(NO2)PhCOCl	0.29		29
I-8	SnO2/en	3,5-(NO2)2PhCOCl	0.96,[g] 0.98, 1.00		48, 49, 50
I-9	SnO2/en	4-FPhCOCl		1.84	77
I-10	RuO2/PrNH2[j]	3,5-(NO2)2PhCOOH[i]	1.48		74
I-11	RuO2/PrNH2[h]	3,5-(NO2)2PhCOCl	0.42, 0.27, 0.33, 0.30		21, 13, 16, 15
I-11a	RuO2/PrNH2[k]	4-(NO2)PhCOCl	0.20		20
I-12	RuO2/en[h]	3,5-(NO2)2PhCOCl	0.49, 0.53, 0.72, 1.35		24, 25, 36, 63
I-13	TiO2/en	3,5-(NO2)2PhCOOH[i]	0.24		12
I-13a	TiO2/en	3-(NO2)PhCH2COOH[i]	0.21		21
I-14	Pt/PtO/en	3,5-(NO2)2PhCOCl	0.45		(23)[l]
I-15	Pt/PtO/en	3,5-(NO2)2PhCOOH[i]	0.45, 0.68		(23, 34)[l]

[a] Electrode/PrNH2 and electrode/en denote surfaces reacted using Method C with 3-aminopropyltriethoxysilane and 3-(2-aminoethylamino)propyltrimethoxysilane, respectively. [b] ESCA data comparing acid and base treatment are on separate specimens to avoid possible beam damage effects. [c] Intensities are in % of total amine band area; actual B.E. in alkylamine-silane doublet are 399 3 eV and 400.6 eV for en and 400.3 eV and 401.9 eV for PrNH2. [d] Percentage of total nitrogen intensity shifted to higher B.E. by acid wash. [e] Percentage of total alkylamine-silane N 1s band (Amine + Amide) which yields tagged derivative. Nitro derivatives normalized according to number of nitro sites; fluoro derivative normalized with cross-section (30) ratio 0.42. [f] Data taken from figure in ref. 7, silanization reaction Method A. [g] Silanization Method D used. [h] Thermal curing post-silanization treatment. [i] Amidization using DCC coupling procedure. [j] Anhydrous post-silanization handling, reactions conducted in glove box. [k] Silanization Method E used. [l] See text.

mensional cross-linking of the surface, expelling H2O and/or ROH to yield siloxane bridges as in Structure V.

V
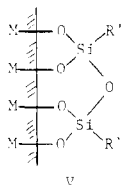
Consequences of these three modes of post-silanization handling have been observed in several experiments. RuO2 and Pt/PtO surfaces after silanization with en silane react with nitrobenzoyl chlorides; the resulting surfaces exhibit electrochemical surface waves characteristic of the nitro-aromatic moiety (2, 3). Differences in the electrochemical behavior were noted on the Pt/PtO surfaces depending on whether the freshly prepared Pt/PtO/en surface was exposed to moisture or not prior to the amidization step (3). This possibly is associated with reactivity of dangling –SiOH groups in the water-exposed samples. An analogous sensitivity of RuO2/en surfaces toward moisture was not observed (2) in the electrochemistry of nitroaromatics immobilized on the RuO2/en electrodes, which had been thermally cured, and which were thus probably in the less reactive Structure V. Effects of thermal curing are also found in tests of stability of RuO2/en surfaces toward hot (ca. 80 °C) water. Freshly silanized RuO2/en is stable in a variety of solvents, but a few minutes' exposure to hot water completely strips the alkyl-amine–silane as evidenced by disappearance of its N 1s spectrum. After curing at 85 °C (in vacuo) for 30 min, 50–60% of the N 1s band survives the hot water test. Involvement of Structure V is implied but not proven by this experiment; whether the hot water degradation is due to –RuOSi– bond

hydrolysis or dissolution of the outermost RuO2 lattice is not known. In contrast to the result on RuO2/en, boiling a SnO2/en electrode for 2 h in water produced no alteration in the observed N 1s or Si 2p spectral intensities. Curing effects on SnO2/en have not been ascertained, and on Pt/PtO/en thermal curing incurs unacceptable and not further investigated increases in electrochemical background currents. These various observations show that the form of post-silanization handling is an experimental variable which merits detailed attention in electrode preparation.

Analysis of Alkyamine-Silanized Metal Oxide Surfaces for Active Amine. Since one intent of alkylamine-silanization is to immobilize amine sites on the metal oxide electrode as reagents for further molecular elaboration of the surface, analysis of the fraction of immobilized nitrogen which actually will react as amine is a relevant measurement. Using ESCA N 1s data, we have measured active amine as proton-atable base, and as amide-forming functionality.

Acid-Base Reactions of Immobilized Alkylamine–Silane. The N 1s band observed on SnO2 electrodes immediately after reaction with alkylamine–silane (Figure 1) and alkylpyridine–silane (1) is a doublet which from the observed binding energies and separation (400.3 and 401.9 eV for PrNH2 and 399.3 and 400.6 eV for en silane) is reasonably interpreted as a mixture of free and protonated amine. Exposure to water or dilute base diminishes but does not eliminate the higher B.E. band (unexpected since a protonated alkylammonium site attached to the metal oxide surface only through the alkyl chain should be deprotonated by this treatment). Also, exposure to strong acid (0.05 M HCl) only partially converts the free base band into the higher B.E. form. These effects are reversible and occur with little change in total N 1s intensity.
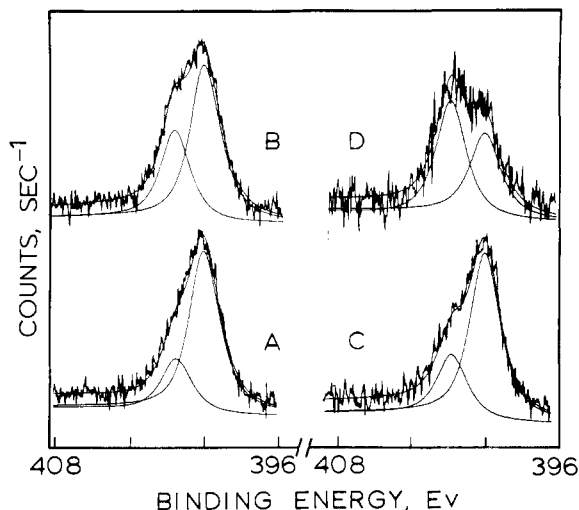
Figure 4. N 1s spectra for $SnO_2/PrNH_2$ (Curves A, B) and SnO_2/en (Curves C, D) electrodes exposed to pH 10 aqueous base (lower) and to 0.05 M HCl (upper) resolved into protonated and free base spectral components. Different samples used for each experiment

Figure 4 shows the N 1s doublet for $SnO_2/PrNH_2$ and SnO_2/en surfaces exposed to aqueous acid and base, and Table I gives areas of the resolved bands (Experiments 1, 2). Taking the relative change in intensity of the higher binding energy band as a measure of active amine, the results indicate that only a small portion of the nitrogen on the $PrNH_2$ silane surface is active base. A larger fraction is active on the SnO_2/en surface. On both surfaces a significant fraction of the nitrogen retains the higher binding energy even upon base wash. RuO_2/en behaves similarly (Experiment 3).

These results suggest three forms of nitrogen on alkyl-amine-silanized metal oxide: a form with free amine binding energy which resists protonation in acid (designated as [N] form), a form with ammonium binding energy which resists deprotonation (designated as [NH] form), and an active, reversibly protonated form (designated as [N/NH] form). Analysis of the data in this manner is subject to criticism as it neglects "transfer" effects (changes in the alkylamine–silane surface in going from an aqueous acid–base equilibrium to a dry state and thence into the vacuum of the electron spectrometer). For example, amine protonated while in contact with the aqueous acid is possibly deprotonated when dried or placed under vacuum, in which case the determined % [N/NH] form is too low and the actual % [N] form is lower than that measured (or non-existent). The lability of the acid–base reaction is a potential liability in the active amine assay. An active amine analysis in which the amine derivatization is more permanent, such as in an amide, is desirable.

**Amidization of Immobilized Alkylamine–Silane.** Amidization of an en or $PrNH_2$ alkylamine-silanized surface with an acid chloride or with a carboxylic acid in the presence of a dehydrating agent such as N,N'-dicyclohexylcarbodiimide (DCC), produces little change in the overall appearance of the alkylamine–silane N 1s doublet. The amide and alkylamine nitrogens have similar binding energies (31). To determine the fraction of amide nitrogen in the unresolved amine + amide band, the amidizing reagent should contain a "tag" atom with distinctive binding energy. For instance, reaction of a $SnO_2/PrNH_2$ surface with 3,5-dinitrobenzoyl chloride yields a nitro N 1s band at 406.5 eV, well resolved from the amine + amide band. The relative intensities of the two bands reflect the extent of amide formation. If the $SnO_2/PrNH_2$ surface consists of 100% active amine, the band area of the nitro band would be 2 × that of the amine + amide band. A different element can alternatively be used for the tag atom, such as F or S. In this case a relative elemental sensitivity

factor becomes included in the active amine determination, which is thereby somewhat less reliable.

Results of such tag atom amidization assays for active amine are given in Table I. Examples of spectra have been reported previously (2, 3). Shake-up bands as observed for nitroanilines (32) or beam damage effects are not seen in the nitro tag spectra or in a spectrum of authentic n-propyl-3,5-dinitro-benzamide, which exhibits a stable nitro/amide N 1s band area ratio of 2/1 as expected.

The experiments on SnO_2 employ several amide reagents since the initial work was done on this material. On a $SnO_2/PrNH_2$ surface, Experiments I-4, 5, and 6 show only 6–27% of the surface nitrogen amidized by the indicated reagents, in contrast with SnO_2/en where 50% amidization is obtained using 3,5-dinitrobenzoyl chloride (Experiment I-8). Note that en silane contains two alkylamine functions, so if one assumes that amidization occurs predominantly at the terminal primary nitrogen, Experiment I-8 results indicate 100% active primary amine for en silane as compared to 6–27% for $PrNH_2$ silane. While the fraction of amine which is active on both en and $PrNH_2$ silanized surfaces is actually dependent on experimental variables as discussed below, the key result is that a lower fraction of primary nitrogen undergoes amidization on $PrNH_2$-silanized surfaces.

Incomplete reactivity of surface nitrogen on $SnO_2/PrNH_2$ and SnO_2/en surfaces can be interpreted in terms of hydrogen-bonding of amine, principally that in the γ position on the alkyl chain, to silanol (–SiOH) functions on the parent or neighbor silane which result from hydrolysis of uncoupled silane. (In most of these experiments, no special precautions were taken to maintain anhydrous post-silanization conditions.) Additionally hydrogen bonding could involve unsilanized metal hydroxyl (–MOH) sites. We suggest that the surface structures may be
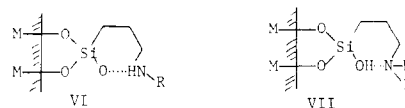
where R = H for $PrNH_2$ and R = $-CH_2CH_2NH_2$ for en silane.

There is considerable precedent in previous silanization work conducted under both polymer forming and anhydrous conditions for this explanation of inactive amine. Hydrogen bonding of amine sites in alkylamine–silanes to silanol or other surface hydroxyls has been widely inferred (33–35). Infrared spectra demonstrate the adsorption of ammonia on silanol groups at silica (36). Kahn (37) obtained evidence for liquid crystal orientations at $PrNH_2$-silanized surfaces from which a parallel orientation of the alkylsilane chain, and hence cyclical bonding of the amine, is implied. Anderson et al. (38) observed a doublet N 1s ESCA band on a polymeric $PrNH_2$ silane coating on silicon and attributed the higher binding energy nitrogen to ammonium sites caused by presence of silanol functions. The results in Table I and the postulated Structures VI and VII are consistent with this background, and demonstrate methodology for a more quantitative description of hydrogen bonding on alkylamine-silanized surfaces than has been previously accomplished.

Depending on steric and solvation effects, the stability of hydrogen bonded Structures VI and VII may vary throughout the surface population. In an amidization assay for active amine, therefore, the unbonded "normal" amine ([N/NH] form) population may be augmented by reaction of some more weakly bonded Structures VI and VII, in which case the active amine assay is not absolute but becomes an apparent and variable quantity which depends on the amidization reagent and the reaction conditions. There is some indication that this may be a considerable effect. For instance, assay results using the 4-nitrobenzoyl, 3,5-dinitrobenzoyl, and 4-fluoro-

benzoyl chlorides on SnO_2/en surfaces vary widely (Experiments I-7, 8, 9). The active amine assayed by 3,5-dinitrobenzoyl chloride on $RuO_2/PrNH_2$ and $SnO_2/PrNH_2$ is normally low (Experiments 4-6, 11), but one experiment using anhydrous post-silanization and DCC coupling conditions gave a high % active amine assay (Experiment I-10). Results on RuO_2/en surfaces (Experiment I-12) indicate a generally higher % active primary amine but are scattered since a range of 3,5-dinitrobenzoyl chloride reaction conditions was employed. Results on $Pt/PtO/en$ are probably erroneously low due to interference from adsorbed amine impurity on this particular oxide. Finally, because of interference from direct adsorption of metal ions by the SnO_2 oxide (1), we are unable to quantitate SnO_2/en reactivity toward metal ion coordination. Whether metal ions are effective in disrupting Structures VI and VII to form en-chelates, on these oxides or on silica (13), is a question specifically unanswered by the present data.

The amidization results generally substantiate the acid–base assay in terms of an unreactive amine population. The hydrogen bonded amines of Structures VI and VII represent the nonprotonatable [N] and nondeprotonatable [NH] forms, respectively, which should exhibit a binding energy difference similar to that between free base and protonated amine. The acid–base results for active amine are lower than those obtained by amidization so the acid–base conditions used are either less reactive at opening Structures VI and VII or do so less permanently (e.g., transfer effects).

Thus, binding of alkylamine–silane to SnO_2 and RuO_2 is thought to involve cyclical hydrogen-bonded structures whose specific reactivity depends both on silane and the assaying reagent. A larger fraction of amine can be induced to undergo amidization on en silane since its terminal primary amine site is less subject to hydrogen-bonding. For this reason the en silane is preferred over $PrNH_2$ silane when high coverages of immobilized redox couples are sought on chemically modified electrodes (2, 3). Also, in the absence of assays such as above, it is risky to assume that reactivity of a surface immobilized chemical functionality is quantitatively the same as its solution counterpart. Perturbing interactions not present in the solution environment can disturb a quantitative parallel.

Alkylamine-Silanized Glassy Carbon: Acid–Base Behavior and Unsuccessful Amidization. Reaction of glassy carbon electrodes with $PrNH_2$ and en silanes in warm dry benzene for ca. 1 h yields surfaces exhibiting N 1s and Si 2p bands more intense than typical background. These surfaces are stable to a variety of organic solvents and, provided they are first thermally cured, to hot water and dilute aqueous acid and base. However, contrary to our previous expectations (4), neither alkylamine-silanized carbon yields evidence of surface amidization using a variety of reagents at room temperature, including 4-nitrobenzoyl, 4-fluorobenzoyl, and 3-bromopropionyl chlorides and 1,1'-ferrocenedicarboxylic acid (DCC procedure). The tag element ESCA band in each attempted amidization was not significantly different from a control (not silanized) electrode. Some loss of amine band intensity was usually noted after reaction. More forcing reaction conditions, e.g., base catalysis or elevated temperatures, resulted in cleavage of silane from the surface. Dithiocarbamate and Schiff base formations were also attempted without success. Alkylamine-silanized glassy carbon does not seem to provide useful coupling chemistry for the preparation of chemically modified carbon electrodes, at least not under monolayer coverage conditions. A different chemical approach is more successful (39).

Alkylamine-silanized glassy carbon does exhibit a protonated/free base amine N 1s doublet (4) similar to that observed on the metal oxide electrodes. Figure 5 illustrates
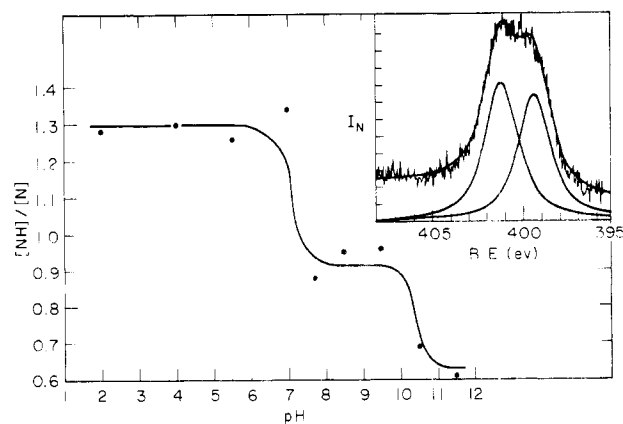

Figure 5. Ratio of protonated and free base (I_{NH}/I_N) N 1s intensities on glassy carbon/en electrodes as a function of pH of aqueous buffer to which the surface was exposed. Inset shows resolving of two N 1s components. Different sample used for each pH point

resolution of this doublet. C/en surfaces were exposed to a series of buffer solutions, the surfaces blown dry with an air jet, and the I_{NH}/I_N intensity ratio measured. Discontinuities in I_{NH}/I_N occur (Figure 5) near the pK values (6.85 and 9.93) (40) of free ethylenediamine. The discontinuities appeared each of several times this experiment was repeated but varied as much as one pK unit. $C/PrNH_2$ surfaces, in contrast, exhibited no change in the I_{NH}/I_N ratio (0.75) over a similar pH range. These results are difficult to interpret cleanly, but could be rationalized in terms of a stable array of surface structures cyclized at the γ-amine site as in Structures VI and VII. The terminal amine of Structure VI in C/en would be more basic than that for Structure VII for the same reason that ordinary ethylenediamine exhibits two different pK values. Thus the titration of Figure 5 would correspond to neutralization of Structures VI and VII. Validity of this tentative model aside, the interesting aspect of Figure 5 is a suggestion that quantitative information on surface acid–base properties may be obtainable using a very primitive solution-to-vacuum transfer. The behavior of the buffer solution as a thin film of it dries on the surface during the transfer may be crucial.

The acid–base behavior of the C/en surface is difficult to reconcile with the lack of success in amidizing the apparent surface amine. It may be that the loss of N 1s intensity upon attempted amidization is associated with cleavage of the active amine form of the en silane from the surface under the reaction conditions. In view of this complication, further experiments like that in Figure 5 will focus on different substrates than carbon.

Analysis of N/Si Surface Atom Ratios. The structural integrity of alkylamine–silanes immobilized on the metal oxide surface is measurable using N/Si ESCA band intensities (area). Table II gives data. Comparing surfaces prepared by reaction with en silane, I_N/I_{Si} data differ between the various metal oxides. The I_N/I_{Si} ratios tend to be low on SnO_2/en surfaces, and to depend there on silanization reaction conditions. I_N/I_{Si} values on SnO_2/en surfaces prepared under the mildest conditions (Experiment II-2, 10 s) are comparable to I_N/I_{Si} data on RuO_2/en and TiO_2/en surfaces prepared using Method C (Experiments II-7, 8, 10). SnO_2/en surfaces prepared under the most forcing silanization conditions (Method A, Experiment II-1) exhibit the lowest I_N/I_{Si} ratios. $Pt/PtO/en$ surfaces exhibit high I_N/I_{Si} ratios.

The quality of the I_N/I_{Si} data is of course influenced by background N 1s and Si 2p bands. Unreacted samples of RuO_2 and TiO_2 are typically free from significant N 1s or Si 2p blanks. On SnO_2, however, a Si 2p background appears at the same B.E. as the silane band, with erratically varying

Table II. N/Si Surface Atom Ratio from ESCA Band Intensities

Alkylamine-Silanized Electrodes

Expt	Electrode	$I_N/I_{Si}{}^a$	Calcd N/Si[b]	N/Si in silane[c]	Silane N/Si/ Calcd N/Si
II-1	SnO_2/en^d	1.09 ± 0.38 (8)	0.60	2	3.33
II-2	SnO_2/en^e				
	(10 s)	2.95	1.62	2	1.23
	(20 s)	2.42	1.33	2	1.50
	(1 min)	2.64	1.45	2	1.38
	(3 min)	1.29	0.71	2	2.82
	(6 min)	1.33	0.73	2	2.74
II-3	SnO_2/en^f	1.34	0.74	2	2.70
II-4	SnO_2/en^g	1.93	1.06	2	1.89
II-5	$RuO_2/PrNH_2{}^h$	1.46 ± 0.10 (4)	0.80	1	1.25
II-6	$RuO_2/PrNH_2{}^i$	1.76 ± 0.09 (4)	0.97	1	1.03
II-7	RuO_2/en^h	2.52 ± 0.36 (2)	1.38	2	1.45
II-8	RuO_2/en^i	2.86	1.57	2	1.27
II-9	$RuO_2/triam^h$	5.77	3.17	3	0.95
II-10	TiO_2/en^h	3.42 ± 0.38 (3)	1.88	2	1.06
II-11	$Pt/PtO/en^h$	7.0 ± 1.0 (6)	4.02	2	0.50
II-12	$Pt/PtO/en^i$	2.70 ± 0.22 (2)^j	1.55	2	1.29

Standard Materials

Expt	Sample	I_N/I_{Si}	Calcd N/Si[b]	Actual N/Si	Actual/calcd
II-13	Si_3N_4	1.74 ± 0.16 (3)	0.96	1.33	1.39
II-14	$PrNH_2$ silane polymer[k]	1.85	1.02	0.91^l	0.89
II-15	en silane polymer[k]	2.78	1.53	1.54^l	1.01
II-16	triam silane polymer[k]	4.55	2.50	3.05^l	1.22

[a] Band area ratios of N 1s at 401.5 ± 400 eV to Si 2p at 102 eV, except for Expts II-11, 12, which used Si 2s at 160 eV to avoid interference with a Pt band. Number of specimens in ( ). [b] Band area ratio converted to atom ratio using sensitivity factor of N/Si of 1.82 to N 1s/Si 2p and 1.74 for N 1s/Si 2s. See text. [c] Stoichiometric atom ratio in the indicated pure silane. [d] Electrodes prepared using silanization Method A. [e] Silanization Method D; data from Figure 1. [f] Silanization Method D. [g] Silanization Method D followed by amidization with 4-$(NO_2)PhCOCl$. [h] Silanization Method C. [i] Silanization Method C followed by amidization with 3,5-$(NO_2)_2PhCOOH$ (DCC). [j] Band area ratio of N 1s at 406 eV to Si 2s at 160 eV and assumption of 50% active amine. [k] Polymer samples prepared from silane by hydrolysis with water, drying, grinding to powder. [l] Polymer sample analysis by Galbraith Laboratories.

intensities (entirely absent on occasional samples and amounting to 50% of the band on a silanized SnO_2 surface in other instances). A background correction was not attempted because of this inconsistent behavior, and the SnO_2/en I_N/I_{Si} are thus known to be low. It is not clear, however, that the Si background problem can account for the systematic variation of SnO_2/en surfaces with silanization reaction conditions. Relative to RuO_2/en and TiO_2/en, then, except for the mild silanization reaction condition, the SnO_2/en surfaces appear qualitatively Si-rich (or N-poor). On Pt/PtO surfaces, no difficulties exist with Si blanks as long as silicon-containing polishing materials are avoided in the Pt electrode resurfacing which follows each experiment. N 1s background bands are seen at ca. 400 eV from time to time but are not typically large enough to cause as high a I_N/I_{Si} as observed on Pt/PtO/en surfaces (Experiment II-11), which seem to be N-rich.

Conversion of I_N/I_{Si} data to N/Si atom ratios involves a relative ESCA elemental sensitivity factor

$$\frac{I_N}{I_{Si}} = \left[\frac{\sigma_N \lambda_N \phi_N}{\sigma_{Si} \lambda_{Si} \phi_{Si}} \right] \frac{T_N C_N D_N}{T_{Si} C_{Si} D_{Si}} \tag{1}$$

where σ is photoionization cross-section for the N 1s and Si $2p_{(1/2+3/2)}$ levels, λ are the escape depths for photoelectrons from these levels, ϕ is the angular correlation factor for photoelectrons at the photon beam-sample-spectrometer acceptance angle, T is spectrometer efficiency for electrons of the given kinetic energies, C is an attenuation factor for adsorbed contaminant hydrocarbon layer on the sample, and D is atom density. Using computed and tabularized (30)

cross-sections $\sigma_N/\sigma_{Si(2p)} = 2.06$; $\phi_N/\phi_{Si(2p)}$ is calculable (41) (equals 1.107 for our spectrometer's 67° angle); and λ_N/λ_{Si} is estimable from the $\lambda\alpha(KE)^{0.75}$ relationship which at $KE \geq 300$ eV is a good approximation (42) to a more exact formulation (43) (equals 0.80 for N 1s/Si 2p). The term in brackets in Equation 1 is thus 1.82 for N 1s/Si 2p. The dispersion of our spectrometer's efficiency with kinetic energy, if any, is not documented. It employs a voltage retarding feature which at the extreme could yield a relation (44) $T\alpha(KE)^{-1}$, which would correspond to $T_N/T_{Si} = 1.35$. Attenuation by the contaminant is also an uncertain factor; if the film is assumed to be ca. 20 Å hydrocarbon, which is probably generous, a very rough calculation gives $C_N/C_{Si} \sim 0.8$ (attenuation is larger for the lower KE N 1s photoelectrons). The last two factors tend to cancel one another, and if we then assume $T_N C_N/T_{Si} C_{Si} \sim 1.0$, the theoretical estimate for the N 1s/Si 2p sensitivity ratio is 1.82.

The N 1s/Si 2p sensitivity ratio was also evaluated with chemical standards. Several materials (not sputtered) are compared to the theoretical value in Table II. Prepared, analyzed (bulk) alkylamine siloxane polymers agree reasonably well with the theoretical value. Data for Si_3N_4 agree less well. Previous (45, 46) sputter profiles of Si_3N_4, however, suggest that its unsputtered surfaces tend to be N-poor. Other available standards work likewise notes a problem with Si data (42). The 1.82 factor was adopted for conversion of I_N/I_{Si} in Table II to N/Si atom ratios, but the reader will note that use of a 1.31 factor from the Si_3N_4 sample would not alter essential features of the following discussion.

Examining RuO_2 electrodes first, the calculated N/Si atom ratios on electrodes silanized with $PrNH_2$, en, and $triam$
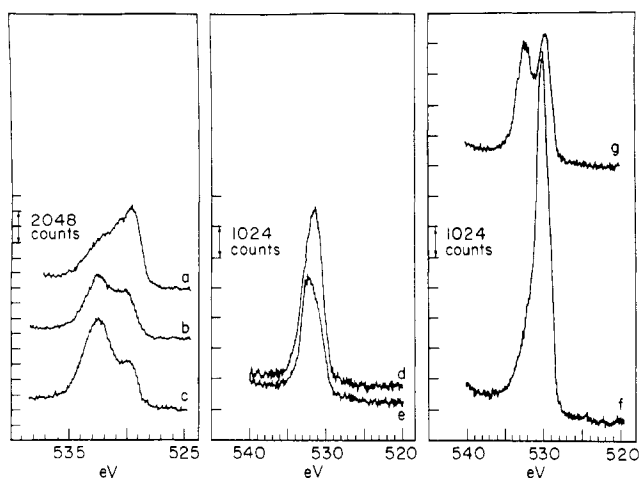
Figure 6. O 1s spectra on various metal oxides. Curve A: RuO_2; Curve B: RuO_2/en; Curve C: $RuO_2/PrNH_2$; Curve D: SnO_2; Curve E: $SnO_2/PrNH_2$; Curve F: TiO_2; Curve G: TiO_2/en

Table III. O 1s Binding Energies

Sample	O 1s B.E., eV[a]		
		Lattice	Source
SnO_2	sh	530.8	This work
	532 (sh)	530.5	(7)
	531.7[b]	530.1	(47)
$SnO_2/PrNH_2$	531.8	sh	This work
SnO_2/en	~531.5	530.8	This work
$SnO_2/PrNH_2$	532	530.5 (sh)	(7)
RuO_2	~532	529.6	This work
RuO_2	530.5 (sh)[c]	529.4	(48)
$RuO_2/PrNH_2$ (or en)	532.1 ± 0.2	529.7 ± 0.2	This work
TiO_2	sh	530.0	This work
TiO_2/en	532.0 ± 0.3	529.8 ± 0.3	This work
Porous silica		532.8	This work
Glass		532.5	This work
Glass fibers		532.4	(55)
Glass		531.2, 529.4[d]	(56)
NiO	531.2[b]	529.4	(50)
CuO	531.6[b]	529.7	(51)

[a] B.E. in this work referenced to C 1s (285 eV); B.E. by others referenced variously to Au, Ag, C 1s, and exact correspondence B.E. cannot be expected. [b] Interpreted variously as chemisorbed oxygen species or surface hydroxyl. [c] Hydrated sample; pure prepared sample has 531.5 band interpreted as RuO_3 defect. [d] Interpreted as "non-bridging oxygen".

silanes are in reasonable agreement with the ideal molecular ratios. The result for TiO_2/en is similar. Structural degradation of the alkylamine–silane does not appear to occur upon binding to these surfaces.

The N/Si atom ratio results for SnO_2/en surfaces, known to involve error from the Si background problem, suggest a nonideal N/Si surface stoichiometry, particularly for surfaces prepared under the more vigorous reaction conditions. Two explanations for silicon-richness on a silanized metal oxide surface can be offered. First, it is possible that the silane reagents contain deaminated trialkoxyalkylsilanes or these are produced by decomposition pathways in the reacting solution. Secondly, the silane reagent may penetrate the outermost, hydrated one or two atomic layers of the SnO_2 lattice, nucleophilic attack by –SnOH on the alkylamine sidechain then occurring to expel that group with its amine nitrogen. The silicon would reside as silicate sites interspersed in the surface SnO_2 lattice, as below

VIII
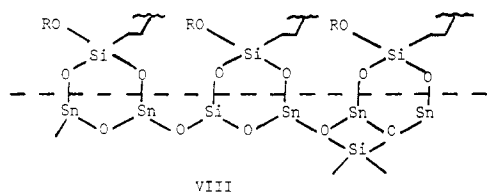
Both explanations for Si-richness are speculations.

The N/Si atom ratio on $Pt/PtO/en$ shows that this surface is N-rich. The Pt/PtO surface differs from the other electrodes in that the oxide layer is an approximate monolayer rather than a bulk oxide (3). This oxide, or patches of exposed Pt^0, may chemisorb amine components from decomposed alkylaminesilane in the reacting solution. If so, the amine + amide N 1s band of Table I is enhanced on Pt/PtO and the active amine assay of Table I (Experiments I-14, 15) is thereby low. Electrochemical experience with the $Pt/PtO/en$ surface suggests fairly high coverages in amidization reactions (3), and the portion of immobilized alkylamine–silane which reacts as active amine may be higher than that represented in Table I by 2× or more. If, for instance, we assume the reactivity of en silane on $Pt/PtO/en$ is like that on SnO_2/en surfaces (e.g., 50% active amine), and then employ I_N/I_{Si} data taken using the 406 eV nitro band on a silanized, amidized electrode (Experiment II-12), an atom ratio more in line with the results on RuO_2/en and TiO_2/en surfaces results. A better-substantiated quantitative picture of the alkylamine–silane stoichiometry on $Pt/PtO/en$ surfaces than this is obviously

desirable but will require further experiments.

Effect of Silanization on O 1s Spectra of Metal Oxides. Each of the three bulk metal oxide electrodes exhibits a dominant O 1s band which is presumably the lattice –MOM– oxygen, and also a higher B.E. O 1s band which is poorly resolved from the main band for SnO_2 (Figure 6, Curve D) but distinct for RuO_2 and TiO_2 (Curves A, F). The SnO_2 shoulder has been observed by others (7, 47), and similar shoulders are common observations (48–54) on other metal oxides especially upon exposure to air and moisture. A collection of metal oxide O 1s data is given in Table III. The higher B.E. shoulder is usually interpreted as surface hydroxyl (7, 47, 50–54) although evidence for a different metal oxidation state was presented for RuO_2 (48).

Reaction of the metal oxide electrodes with an organosilane produces a much more prominent higher B.E. O 1s band (Curves B, C, E, G, Figure 6). The B.E. of this band is approximately the same for $PrNH_2$ and en-silanized surfaces, and on RuO_2 and TiO_2, where accurate B.E. measurements were feasible. The intensity of the higher B.E. band roughly correlates with the intensity of the N 1s band of the alkylamine–silane and thus it is related to coverage achieved in the silanization reaction. It is particularly intense on samples bearing siloxane polymer. The lattice O 1s band exhibits no change in B.E. upon silanization but is lowered in intensity presumably because of photoelectron scattering by the overlying silane.

The higher B.E. O 1s band which appears upon silanization can be interpreted as –MOSi– oxygen, (although contributions from –SiOH, –SiOR, or adsorbed water are also possibilities). The lattice O 1s band for –SiOSi– bound oxygen (as in silica) lies at higher B.E. (by 2–3 eV, see data in Table III) than the typical lattice oxygen in the more ionic metal oxides. The band on silanized metal oxide has an intermediate B.E.; compare 530.0 eV for TiO_2 lattice O 1s and 532.5 eV for glass (our data) with the observed 532.0 eV on TiO_2/en. This would qualitatively be expected for –MOSi– oxygen. The –MOSi– band overlies or supplants by reaction the surface hydroxyl present on the metal oxide before silanization. In the case of SnO_2, care must be taken to avoid specimens with surface Si contaminant when examining the effects of silanization.
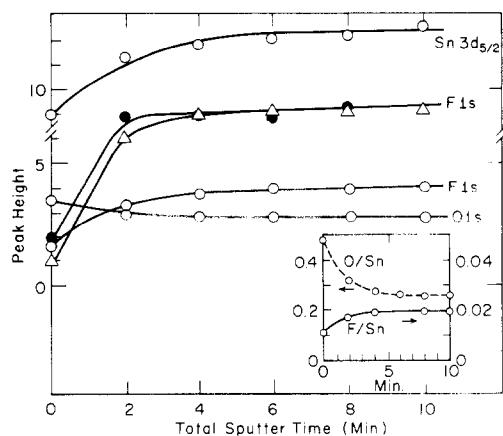
Figure 7. 1.5 eV Ar$^+$ sputter profile for SnO$_2$ (Specimen I, -●-, and specimen II, -O-) and SnO$_2$/en Method D, Specimen III, -△-) electrodes for O 1s, Sn 3d$_{5/2}$, and F 1s. Sputter profiles are on arbitrary intensity scales different for each element; band intensity ratios in inset are actual band areas

The O 1s spectral region has potential qualitative usefulness in study of silanization reactions. We regard quantitative interpretations of intensities as tenuous because of the metal hydroxyl feature and the presence of surface water, adsorption of which is conceivably enhanced by the presence of the silane.

SnO$_2$ Dopant Concentration and Depth Profile. SnO$_2$, an n-type semiconductor in pure form, is useful as a non-rectifying working electrode at positive potentials only when doped with high levels of appropriate carriers. The SnO$_2$ electrodes employed here are fluoride doped; a F 1s band can be detected for this at B.E. 687 eV. The dopant concentration and depth profile are of interest. Figure 7 shows Ar$^+$ sputter profiles for two native SnO$_2$ and one silanized SnO$_2$ electrodes. The variation of I_F with sputter time indicates that the outermost 10-20 Å of the SnO$_2$ electrode is depleted in dopant. The degree of depletion varies with the electrode as does the interior level of dopant. There is no obvious dependence on the electrode having been subjected to silanization. Applying Equation 1 in the same manner as for N/Si, a relative sensitivity factor of 0.26 is used to convert the I_F/I_{Sn} band area ratios (Figure inset) for Specimen II at zero sputtering time (surface) and 10-min sputtering time (interior) to F/Sn atom ratios of 0.034 and 0.056, respectively. These are approximate values since I_F for Specimen I, for instance, was twice as large, and also the relative sensitivity factor was not compared to standards. Using 6.95 g·cm^3 for SnO$_2$ density, carrier populations of 9.4×10^{20} and 1.6×10^{21} atoms/cm^3 are calculated for the SnO$_2$ surface and bulk, respectively. The surface carrier population is sufficiently high that adverse electrochemical properties are not expected from the depletion effect, and importantly the depletion effect is not enhanced by the silanization reaction.

The dopant depletion for SnO$_2$ is in contrast to Sn-doped In$_2$O$_3$, which according to Kuwana exhibits a higher Sn/In ratio at the surface of this electrode material than in its bulk (57).

Figure 7 also shows a variation of I_O/I_{Sn} (band areas) with Ar$^+$ sputtering similar to a previous measurement (57). The F dopant depletion falls within the region of enhanced I_O/I_{Sn}, which we interpret as a layer of partially hydrated SnO$_2$ lattice, for the following reasons. Using a relative O/Sn sensitivity factor 0.20 derived from Equation 1, the calculated O/Sn atom ratio for SnO$_2$ electrodes varies typically from 2.4 prior to sputtering to about 1.4 after sputtering attains a constant I_O/I_{Sn}. (One sample gave an initial O/Sn ratio of 3.5, but the same final value.) These calculations, by themselves, suggest that while the outermost surface is hydrated, the Ar$^+$ beam sputtering induces a chemical change in the SnO$_2$ to a lower

oxide form and so the actual depth of lattice hydration is less than the profile of Figure 7 implies. The possibility of reduction during sputtering of SnO$_2$ powder has been advanced (47). In an alternate interpretation, using an emperical relative O/Sn sensitivity factor 0.11 (58) with Figure 7 yields O/Sn atom ratios typically 4.3 before sputtering and 2.5 after. This calculation suggests even more extensive surface hydration and little or no Ar$^+$ reduction effect. A sputtering experiment with 400 eV Ar$^+$ was stated elsewhere not to cause reduction of SnO$_2$ (59). Lastly, we have observed an example of metal ion chemisorption (60) to the same depths as the I_O/I_{Sn} variation. The evidence supports our interpretation of Figure 7 in terms of a hydration deeper than the outermost SnO$_2$ lattice plane.

DISCUSSION

For the most part, the above results show that the alkyl-amine-silanized surfaces exhibit expected and understandable properties, and the hope of chemical amine-like predictability of the modified metal oxide electrode surface is qualitatively realized. The alkylamine-silanized interface cannot, on the other hand, be considered as solely an amine-like surface; its chemistry is more complex than this. This is not surprising for a surface synthesized under conditions far from the atomically clean single crystal domain. Such chemical complexity will probably be common for other forms of electrode surface modification upon examination on a comparable level of detail.

The motivation for our study of the alkylamine-silanized interface is in its use as a connecting bridge for immobilization of redox reagents on electrode surfaces. We should consider how the present results relate to that application. The alkylamine–silane chain is not itself a good electron transport bridge between immobilized redox reagent and electrode. The length of a bonded en silane from metal to primary amine nitrogen is $\sim$12 Å in extended form and $\sim$9 Å in the hydrogen bonded Structure VII. Unless the activation barrier for electron transfer over such distance proves to be modest, flexible motions of the alkylamine–silane chain will play a role in the electron transfer process. The premise of the so-called "floppy model" (2, 24) is that such flexibility will exist in these modified surfaces. At least three factors are involved, the frequency of the motion, which will influence the pre-exponential kinetic factor (maximum value $kT/h \sim 10^{13}$ s^{-1}) (61, 62), and the distance and geometry of redox reagent approach to metal oxide, which will influence $\Delta G^\ddagger$. Motions of the alkylamine–silane chain will be affected by Structures I–III, V, VI, and VII. Overall stability of the modified surface is enhanced by multiple –MOSi– bonds, and by cross-linking as in Structure V, but motional freedom of the amine site diminishes in the order of Structures I > II > III. We conjectured that I and II are more likely, but no quantitative analysis of this bonding problem is available. Structures VI and VII provide a shorter connecting bridge but also tend to restrain the approach distance. It would appear from the amidization data that the hydrogen-bonded structures may be prevalent in alkylamine–silanes with γ-amine sites. For purposes of modeling of electron-transfer events, then, combinations of Structures I and II with VI and VII probably present a good estimate of the average surface stereochemistry. A considerable complication in such modeling, however, is the possibility that very rapid electron transfer is to but a small population of sites possessing optimum alkylamine–silane chain flexibility. Subsequent *lateral* propagation of electron transfer to other more motionally restricted sites then might actually be the controlling mechanism. Quantitative modeling is tenuous until such eventualities are evaluated.

Our interpretation of the ESCA results indicates that a variety of surface structures may exist within a single specimen

of alkylamine–silanized metal oxide electrode. We can draw from this the intimation that a redox reagent bound to the alkylamine–silane may find itself in a spectrum of slightly different chemical environments. The redox reagent may as a consequence exhibit a spectrum of formal electrochemical potentials, which in turn has the effect of broadening the electrochemical surface wave observed for the reagent. To what extent broadening we have observed in surface waves on alkylamine–silanized electrodes is due to this chemical heterogeneity as opposed to interactive effects within the chemically bound layer (62) or to both, remains to be resolved.

ACKNOWLEDGMENT

LITERATURE CITED

(1) P. R. Moses, L. Wier, and R. W. Murray, *Anal. Chem.*, **47**, 1882 (1975).
(2) P. R. Moses and R. W. Murray, *J. Electroanal. Chem.*, **77**, 393 (1977).
(3) J. R. Lenhard and R. W. Murray, *J. Electroanal. Chem.*, **78**, 195 (1977), A. Diaz, *J. Am. Chem. Soc.*, **99**, 5838 (1977); G. J. Leigh and C. J. Pickett, *J. Chem. Soc., Dalton Trans.*, 1797 (1977).
(4) C. M. Elliott and R. W. Murray, *Anal. Chem.*, **48**, 1247 (1976).
(5) P. R. Moses, J. C. Lennox, J. Lenhard, and R. W. Murray, 173rd National Meeting, American Chemical Society, New Orleans, La., March 1977.
(6) D. F. Untereker, J. C. Lennox, L. M. Wier, P. R. Moses, and R. W. Murray, *J. Electroanal. Chem.*, **81**, 309 (1977).
(7) M. Fujihira, T. Matsue, and T. Osa, *Chem. Lett.*, 875 (1976).
(8) D. F. Untereker, P. R. Moses, L. M. Wier, C. M. Elliott, and R. W. Murray, 149th Electrochemical Society Meeting, Washington, D.C., May 1976.
(9) E. Grushka, Ed., "Bonded Stationary Phases in Chromatography", Ann Arbor Science Publications, Ann Arbor, Mich., 1974.
(10) C. H. Lochmuller and C. W. Amoss, *J. Chromatogr.*, **108**, 85 (1975).
(11) E. Grushka and E. J. Kikta, Jr., *Anal. Chem.*, **46**, 1370 (1974).
(12) H. H. Weetall, *Sep. Purif. Methods*, **2**, 199 (1973).
(13) D. M. Hercules, L. E. Cox, S. Onisick, G. D. Nichols, and J. C. Carver, *Anal. Chem.*, **45**, 1973 (1973).
(14) D. E. Leyden and G. H. Luttrell, *Anal. Chem.*, **47**, 1612 (1975).
(15) R. L. Burwell, *Chem. Technol.*, 370 (1974).
(16) E. P. Plueddemann, *Adhes. Age*, **18**, 36 (1975); *Chem. Abstr.*, **83**, 148735 (1975).
(17) K. Hardee and A. J. Bard, *J. Electrochem. Soc.*, **122**, 739 (1975).
(18) C. N. Reilley and W. S. Woodward, to be submitted for publication.
(19) H. P. Boehm, "Chemical Identification of Surface Groups," *Adv. Catal.*, **16**, 179 (1966).
(20) R. K. Gilpin and M. F. Burke, *Anal. Chem.*, **45**, 1383 (1973).
(21) E. W. Thornton and P. G. Harrison, *J. Chem. Soc. Faraday Trans. 1*, **71**, 461 (1975).
(22) D. J. C. Yates, *J. Phys. Chem.*, **65**, 746 (1961).
(23) H. Kuhn, "Spectroscopy of Monolayer Assemblies", in "Physical Methods of Chemistry", A. Weissberger and B. Rossiter, Ed., Wiley, New York, N.Y., 1972, Part IIIB, p 577.
(24) P. R. Moses and R. W. Murray, *J. Am. Chem. Soc.*, **98**, 1435 (1976).
(25) M. Gleria and R. Memming, *Z. Phys. Chem. (Frankfurt am Main)*, **98**, 303 (1975).
(26) A. A. Oswald, L. L. Murrel, and L. J. Boucher, *Am. Chem. Soc., Div. Pet. Chem., Abstr.*, 168th National Meeting, American Chemical Society, Los Angeles, Calif., 1974.
(27) P. G. Harrison and E. W. Thornton, *J. Chem. Soc., Faraday Trans. 1*, 1310 (1976).
(28) A. Diaz, *J. Am. Chem. Soc.*, **99**, 6780 (1977).
(29) V. S. Srinivasan and W. J. Lamb, *Anal. Chem.*, **49**, 1639 (1977).
(30) J. H. Scofield, Lawrence Livermore Laboratory Report No. UCRL-51326, January 1973.
(31) D. M. Hercules, *Anal. Chem.*, **42** (1), 20A (1970).
(32) S. Pignataro and G. Distefano, *J. Electron Spectrosc. Relat. Phenom.*, **2**, 171 (1973).
(33) H. F. Weetall and L. S. Hersh, *Biochim. Biophys. Acta*, **206**, 54 (1970).
(34) L. Lee, *J. Colloid Interface Sci.*, **27**, 751 (1968).
(35) E. P. Plueddeman, *J. Adhes.*, **2**, 184 (1970).
(36) M. L. Hair, "Infrared Spectroscopy in Surface Chemistry", M. Dekker, New York, N.Y., 1967, p 102.
(37) F. J. Kahn, *Appl. Phys. Lett.*, **22**, 386 (1973).
(38) H. R. Anderson, F. M. Fowkes, and F. H. Hielscher, *J. Polm. Sci., Polym. Phys. Ed.*, **14**, 879 (1976).
(39) J. C. Lennox and R. W. Murray, *J. Electroanal. Chem.*, **78**, 195 (1977).
(40) J. N. Butler, "Ionic Equilibria", Addison Wesley, Reading, Mass., 1964, p 466.
(41) R. F. Reilman, A. Msezane, and S. T Manson, *J. Electron Spectrosc. Relat. Phenom.*, **8**, 389 (1976).
(42) C. D. Wagner, *Anal. Chem.*, **49**, 1282 (1977).
(43) D. R. Penn, *J. Electron Spectrosc. Relat. Phenom.*, **9**, 29 (1976).
(44) J. C. Helmer and N. H. Weichert, *Appl. Phys. Lett.*, **13**, 266 (1968).
(45) J. S. Johannessen, W. E. Spicer, and Y. E. Strausser, *Thin Solid Films*, **32**, 311 (1976).
(46) P. H. Holloway, and H. J. Stein, *J. Electrochem. Soc.*, **123**, 723 (1976).
(47) A. W. C. Lin, N. R. Armstrong, and T. Kuwana, private communication, March 1977.
(48) K. S. Kim and N. Winograd, *J. Catal.*, **35**, 66 (1974).
(49) N. S. McIntyre and M. G. Cook, *Anal. Chem.*, **47**, 2208 (1975).
(50) W. Dianis and J. E. Lester, *Surf. Sci.*, **43**, 602 (1974).
(51) T. Robert, M. Bartel, and G. Offergeld, *Surf. Sci.*, **33**, 123 (1972).
(52) K. S. Kim, A. F. Gossmann, and N. Winograd, *Anal. Chem.*, **46**, 197 (1974).
(53) G. C. Allen, M. T. Curtis, A. J. Hooper, and P. M. Tucker, *J. Chem. Soc., Dalton Trans.*, 1525 (1974).
(54) K. Kishi and S. Ikeda, *Bull. Chem. Soc. Jpn.*, **46**, 341 (1973).
(55) J. P. Rynd and A. K. Rastogi, *Surf. Sci.*, **48**, 22 (1975).
(56) S. R. Nagel, J. Tauc, and B. G. Bagley, *Solid State Commun.*, **20**, 245 (1976).
(57) N. R. Armstrong, A. W. C. Lin, M. Fujihira, and T. Kuwana, *Anal. Chem.*, **48**, 741 (1976).
(58) C. D. Wagner, *Anal. Chem.*, **44**, 1050 (1972).
(59) K. S. Kim, W. E. Baitinger, J. W. Amy, and N. Winograd, *J. Electron Spectrosc. Relat. Phenom.*, **5**, 351 (1974).
(60) L. Wier, unpublished results, Univeristy of North Carolina, 1976.
(61) R. C. Baetzoldanel and G. A. Somorjai, *J. Catal.*, **45**, 94 (1976).
(62) F. C. Anson, U.S.–Japan Seminar, San Francisco, Calif, May 1977.

Analysis of Commercial Sodium Tripolyphosphates by Phosphorus-31 Fourier Transform Nuclear Magnetic Resonance Spectrometry

Stanley A. Sojka* and Roger A. Wolfe

Hooker Chemicals and Plastics Corporation, Research Center, Grand Island Complex, M.P.O. Box 8, Niagara Falls, New York 14302

Commercial sodium tripolyphosphate samples were analyzed by phosphorus-31 Fourier transform nuclear magnetic resonance spectrometry. The accuracy and precision of the method were assessed and found to be satisfactory. Identification of phosphorus-containing species was possible. In some cases, the presence of high polyphosphates interfered with the analysis.

The Fourier transform (FT) approach (1) has added new

dimensions to ^{31}P NMR spectrometry. The time savings and sensitivity enhancement inherent in the FT approach have been realized in practice, and analytical applications are becoming increasingly apparent (2). Detection of organophosphorus compounds at the level of the parts-per-million range has been reported (3). This paper describes the use of ^{31}P FT NMR spectrometry to analyze commercial samples of sodium tripolyphosphate (4, 5), including the determination of accuracy and precision. The advantages of this approach over other analytical procedures, such as gel chromatography